Applications of g-C3N4-Based Photocatalysts

Subjects: Chemistry, Physical

Contributor: Hao Lin, Yao Xiao, Aixia Geng, Huiting Bi, Xiao Xu, Xuelian Xu, Junjiang Zhu

The assembly of g-C_3N_4 with metal oxides is an effective strategy which can not only improve electron–hole separation efficiency by forming a polymer–inorganic heterojunction, but also compensate for the redox capabilities of g-C_3N_4 owing to the varied oxidation states of metal ions, enhancing its photocatalytic performance. Applications of g-C_3N_4-based materials in photocatalysis are discussed, including water splitting to generate H_2 and O_2, the degradation of pollutants, CO_2 reduction and bacterial disinfection.

Keywords: g-C3N4 ; water ; synthesis

1. Photocatalytic Water Splitting for H_2

Because of the decreasing storage of fossil fuels and their negative impacts on the environment (releasing CO_2 for example), the use of green and renewable hydrogen fuels attracts much attention from scientists. The photocatalytic splitting of water is an ideal way to generate hydrogen and has become a hot topic in recent years. **Figure 1** presents a simplified diagram of splitting water into hydrogen and oxygen over g-C_3N_4 under light irradiation. First, g-C_3N_4 is excited by photons to generate electrons, which then jump to the CB, leaving holes at the VB. The photogenerated e^- and h^+ flow to the surface of g-C_3N_4, reducing and oxidizing the adsorbed water to hydrogen and oxygen, respectively. However, the generated e^-/h^+ will rapidly recombine each other due to the Coulombic attraction, losing activity. The improvement in the separation efficiency of the photogenerated e^-/h^+ pairs, thus, is a challenging topic in the field of g-C_3N_4 photocatalysis.

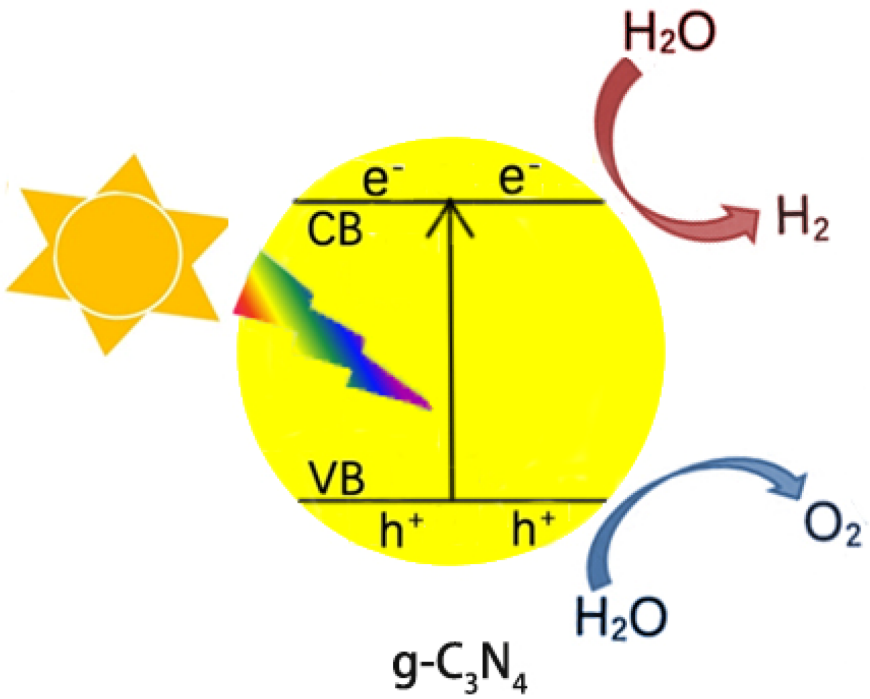

Figure 1. Scheme of photocatalytic water splitting into H_2 and O_2 over g-C_3N_4 under light irradiation.

To achieve this, the coupling of g-C_3N_4 with metal oxide is a solution, which can separate e^-/h^+ pairs in space by forming an opposite flow of e^- and h^+ (for type II heterojunctions), or by inducing the recombination of unused e^- and h^+ (for Z-Scheme heterojunctions), as reported in the literature [1][2]. Shi et al. [3] reported the in situ synthesis of MoO_3/g-C_3N_4, via co-pyrolysis of MoS_2 and melamine, for photocatalytic water splitting to hydrogen, finding that the activity of g-C_3N_4 was significantly enhanced with the increase in MoO_3 content. It is possible that the use of layered MoS_2 as a precursor not only improves the dispersion of MoO_3 on g-C_3N_4, but also enhances the interactions between them. Li et al. [4] synthesized $W_{18}O_{49}$/g-C_3N_4 composites by roasting a g-C_3N_4-impregnated ammonium tungstate solution. The loading of

$W_{18}O_{49}$ greatly improves the surface area (by about five times) and exhibits excellent activity for a photocatalytic hydrogen evolution reaction, with a reaction rate of 912.3 μmol·g^{-1}·h^{-1}, which is 9.7 times higher than that of g-C_3N_4.

The coupling of g-C_3N_4 with two metal oxides could be more interesting when compared to that with single-metal oxide, as multiple heterojunctions can be established, exhibiting rich optical properties, and hence, better photocatalytic activities. This is observed in many studies [5][6][7]. For example, Wang et al. [8] found that Fe_2O_3@MnO_2 core-shell g-C_3N_4 ternary composites can form double heterojunctions, which provide abundant channels for electrons transfer, exhibit enhanced optical properties and allow the two half-reactions (the production of hydrogen and oxygen) to occur on the opposite surfaces of the semiconductor ; this results in improved activity for both hydrogen and oxygen production, with an optimal reaction rate of 124 μmol·h^{-1} and 60 μmol·h^{-1}, respectively.

2. Photocatalytic Reduction of CO_2 to Renewable Hydrocarbon Fuels

With increasing global warming, it is critical to find effective ways to deal with greenhouse gases. Carbon dioxide (CO_2) is not only a typical greenhouse gas but also a valuable C1 resource. Hence, utilizing solar energy to reduce CO_2 into higher-value chemicals shows great advantages in solving the problems of both global warming and energy crises. In the past few years, g-C_3N_4 has been employed as a photocatalyst for CO_2 reduction owing to its high CB potential, which can activate CO_2 by donating electrons to the unoccupied orbits of CO_2. The photocatalytic CO_2 reduction involves a proton-assisted multi-electron process, as shown in Equations (1)–(5) below [9]. From the viewpoint of thermodynamics, CO_2 is gradually reduced to HCOOH, CO, HCHO, CH_3OH and CH_4 by receiving multiple (2, 2, 4, 6 and 8) electrons and protons, accompanying the increase in reduction potential. This means that the photocatalyst used to reduce CO_2 should have strong redox capability in order to supply sufficient driving force for the reaction.

$$\begin{gathered}\mathrm{CO_2 + 2H^+ + 2e^- \rightarrow HCOOH} \\ E^0{}_{\mathrm{redox}} = -0.6\mathrm{V\ (vs.\ NHE\ at\ pH\ 7)}\end{gathered} \tag{1}$$

$$\begin{gathered}\mathrm{CO_2 + 2H^+ + 2e^- \rightarrow CO} + H_2O \\ E^0{}_{\mathrm{redox}} = -0.53\mathrm{V\ (vs.\ NHE\ at\ pH\ 7)}\end{gathered} \tag{2}$$

$$\begin{gathered}\mathrm{CO_2 + 4H^+ + 4e^- \rightarrow HCHO} + H_2O \\ E^0{}_{\mathrm{redox}} = -0.48\mathrm{V\ (vs.\ NHE\ at\ pH\ 7)}\end{gathered} \tag{3}$$

$$\begin{gathered}\mathrm{CO_2 + 6H^+ + 6e^- \rightarrow CH_3\,OH} + H_2O \\ E^0{}_{\mathrm{redox}} = -0.38\mathrm{V\ (vs.\ NHE\ at\ pH\ 7)}\end{gathered} \tag{4}$$

$$\begin{gathered}\mathrm{CO_2 + 8H^+ + 8e^- \rightarrow CH_4} + {}_2H_2O \\ E^0{}_{\mathrm{redox}} = -0.24\mathrm{V\ (vs.\ NHE\ at\ pH\ 7)}\end{gathered} \tag{5}$$

ZnO can absorb CO_2 and has a CB potential (E_{CB}) of −0.44 eV, which is more negative than the reduction potential of CO_2. Therefore, the combination of ZnO and g-C_3N_4 would benefit the CO_2 reduction reaction. Indeed, it is found that although the deposition of ZnO has negligible effects on the light absorption capacity and surface area of g-C_3N_4, the ZnO/g-C_3N_4 composite shows better photocatalytic activity for CO_2 reduction than individual ZnO and g-C_3N_4, due to the formation of heterojunctions that facilitate the separation of e^-/h^+ pairs [10]. The CO_2 conversion rate obtained from ZnO/g-C_3N_4 reaches 45.6 μmol/g/h, which is 4.9 times and 6.4 times higher than that obtained from g-C_3N_4 and P25, respectively. Additionally, based on the fact that the zeta potential of ZnO is positive and that of g-C_3N_4 is negative, Nie et al. [11] constructed a ZnO/g-C_3N_4 composite using an electrostatic self-assembly method. The combination of them induces synergistic effects that are conducive to photocatalytic reactions, in which the ZnO microsphere prevents falling g-C_3N_4 nano flakes from gathering, and the g-C_3N_4 improves light utilization efficiency through the multi-scattering effect.

In addition to ZnO, many other metal oxides can couple with g-C_3N_4 and contribute to the CO_2 reduction reaction. For example, Bhosale et al. [12] employed a wet chemical method to couple $FeWO_4$ with g-C_3N_4, forming a Z-scheme g-

$C_3N_4/FeWO_4$ photocatalyst; it showed good activity for the reduction of CO_2 to CO without any medium, with a CO production rate of 6 μmol/g/h, which is 6 and 15 times higher than that of individual g-C_3N_4 and $FeWO_4$.

3. Photocatalytic Degradation of Pollutants

With the rapid development of the economy, various toxic pollutants emitted from industrial plants have been discharged to the environment and have seriously destroyed the ecological system. The removal of pollutants and the remediation of the environment have thus become essential topics and have attracted broad attention in recent years. Photocatalysis is a prospective technology for pollutant removal, and is able to mineralize organic pollutants into CO_2 and H_2O by producing oxidizing intermediates (such as $\bullet O_2^-$, •OH and h^+). Depending on the properties of the pollutants, three reaction types can be classified: (1) the removal of organic pollutants in aqueous solution, such as dye [4][13] and antibiotic degradation [14]; (2) the removal of heavy-metal cations in aqueous solution, such as the reduction of chromium (VI) [15]; and (3) the removal of organic or inorganic pollutants in gas phase, such as the degradation of ortho-dichlorobenzene [16], acetaldehyde [17] and nitric oxide [18].

The Fenton advanced oxidation process (with an Fe^{2+} and H_2O_2 system) is a traditional technology used to treat industrial wastewater, but it is limited to a narrow pH range (<3) and causes secondary pollution due to the production of iron sludge. For this reason, it is proposed that a photocatalyst should be used instead of Fe^{2+}, to activate H_2O_2 into •OH radicals under light irradiation conditions, which can be achieved in a wide pH range without producing secondary pollutants. Hence, it is a green route to removing organic pollutants in aqueous solution and has good prospects for industrial use.

In this respect, Xu et al. [19] recently reported that the LFO@CN photocatalyst is highly efficient for the oxidative degradation of RhB with H_2O_2 under visible-light irradiation, with 98% conversion obtained within 25 min, and the material can be recycled for four cycles with no appreciable deactivation. Moreover, when applying a ternary $LaFe_{0.5}Co_{0.5}O_3$/Ag/g-C_3N_4 heterojunction that consists of a redox part $LaFe_{0.5}Co_{0.5}O_3$ (LFCO), photo part g-C_3N_4 and plasmonic part (Ag), for the degradation of tetracycline hydrochloride (TC), in the presence of H_2O_2 and light irradiation, the system exhibits good activity due to a photo-Fenton effect induced in the reaction. In this system, H_2O_2 is first activated into •OH radicals and OH^- anions over the LFCO, and the OH^- anions subsequently react with holes (h^+) produced at the VB band of LFCO to form more •OH radicals. Hence, H_2O_2 can be fully utilized to oxidize TC in the reaction. Meanwhile, the O_2 dissolved in the solution can react with the electrons (e^-) generated at the CB band of g-C_3N_4 and form $\bullet O_2^-$, which is also a strong oxidant that is able to oxidize TC into CO_2 and H_2O. These results support that g-C_3N_4-based catalysts have good chemical stability and can be an effective substitute for Fenton catalysts in environmental purification.

In addition to the direct addition of H_2O_2, the photocatalytic in situ generation of H_2O_2 in the reaction for pollutant oxidation, which is a more promising way but a more challenging topic, is also possible. For example, Xu et al. reported that ternary g-$C_3N_4/Co_3O_4/Ag_2O$ heterojunctions can accelerate the mineralization of RhB due to the presence of H_2O_2 in situ, produced from O_2 reduction [20]. Through studying the catalytic behavior of the composites in the electrochemical oxygen reduction reaction (ORR), they found that the average number of electrons transferred in the reaction is 2.07, which indicates that the two-electron O_2 reduction process is the dominant step in the reaction.

The morphology of metal oxide, the interface interaction between metal oxide and g-C_3N_4 and the method of coupling metal oxide with g-C_3N_4 are also crucial factors affecting the photocatalytic performance of g-C_3N_4 for pollutant removal. For instance, the coupling of cubic CeO_2 (3~10 nm) with g-C_3N_4 using a hydrothermal method can greatly improve the activity of g-C_3N_4 for methyl orange degradation, with the reaction rate reaching 1.27 min^{-1}, which is 7.8 times higher than that of g-C_3N_4 alone (0.16 min^{-1}) [21]. The hybridization of NiO with g-C_3N_4 causes a red shift in the UV absorption edge and boosts the ability of light response; hence, it exhibits improved activity for methylene blue degradation, which is about 2.3 times higher than that of g-C_3N_4 [22]. Similar phenomena are also observed for other materials, e.g., TiO_2-In_2O_3@g-C_3N_4 [23].

The heavy-metal ions produced in electroplating, metallurgy, printing and dyeing, medicine and other industries cause serious damage to the ecological environment. Cr(VI) is a typical heavy metal in wastewater and its removal receives wide attention. The photocatalytic reduction of Cr(VI) to Cr(III) is an efficient way to treat Cr(VI)-containing wastewater, due to its simple process, energy savings, high efficiency and lower levels of secondary pollution [24]. It has been reported that the in situ self-assembly of g-C_3N_4/WO_3 in different organic acid media can lead to various surface morphologies and catalytic activities for Cr(VI) removal, as the number of carboxyl groups in organic acid greatly affects the shape and performance of g-C_3N_4/WO_3. Its synthesis in ethanedioic acid medium, which contains two carboxyl groups, yields a disc

shape and has the best activity for nitroaromatic reduction. Furthermore, the material has good stability for the reaction, with no appreciable activity loss within four cycles.

Bi_2WO_6 is a promising semiconductor that can couple with g-C_3N_4 and form a heterojunction for the photocatalytic treatment of Cr(VI)-containing wastewater. Song et al. [25] found that a C_3N_4/Bi_2WO_6 composite prepared using a hydrothermal method exhibits a surface area up to 46.3 m^2/g and shows a rate constant of 0.0414 min^{-1} for the photocatalytic reduction of Cr(VI), as the high surface area of the catalyst facilitates not only the reactant's adsorption, but also the visible-light absorption.

Photocatalysis is also effective for removing gas-phase pollutants and receives great interest from scientists. It is known that air pollution is a big problem for the environment, and causes serious harm to the human body and ecological systems by forming acid rain, chemical smog, particulate matter, etc. Hence, seeking an effective and feasible technology for its removal is a challenging topic. Photocatalysis provides a way to remove air pollutants (e.g., NOx) by installing catalysts either inside the exhaust pipe or on the road surface [26]. As a typical photocatalyst, g-C_3N_4-based materials are also widely investigated in this aspect. Zhu et al. reported that g-C_3N_4 is active in NO removal via thermal catalysis, and proposed that the N atoms of g-C_3N_4, with a lone electron pair, serve as the active site of NO by donating electrons to weaken the N-O bond order [27]. This lays the foundation or using photocatalysis for NO removal, as electrons can be effectively excited from g-C_3N_4 under light irradiation.

However, it is known that the surface area of g-C_3N_4 prepared using the thermal condensation method is small, which grfieatly limits the light absorption capacity, the e^-/h^+ separation efficiency and other physicochemical properties; thus, many strategies have been adopted to overcome this problem. For example, Sano et al. [28] reported that pretreating melamine with NaOH solution before the condensation process favors the hydrolysis of unstable domains and the generation of mesopores in the structure of g-C_3N_4, leading to an increase in surface area from 7.7 m^2/g to 65 m^2/g, and the NO oxidation activity is accordingly increased 8.6 times. Duan et al. [18] found that flower-like g-C_3N_4 prepared using the self-assembly method can notably improve photocatalytic activity for NO oxidation compared to bulk g-C_3N_4, owing to the enlargement of the BET surface area, the formation of nitrogen vacancies, the condensation of π–π layer stacking, and the improvement in e^-/h^+ separation efficiency. The alternation of the precursor, e.g., urea [29] and guanidine hydrochloride [30] is also efficient in preparing g-C_3N_4 with a large surface area and improving photocatalytic performance.

4. Sterilization and Disinfection

In addition to the above applications, photocatalysis is also widely applied to inactivate pathogens in surface water owing to its broad compatibility, long durability, anti-drug resistance and thorough sterilization [31]. Bacteria, such as salmonella, staphylococcus aureus and bacillus anthracis, are commonly used as model pathogens to evaluate photocatalytic disinfection efficiency. Since the first work of Matsunaga et al. [32] on photochemical sterilization in 1985, this technique has rapidly developed and receives great interest from scientists. The principle of photocatalytic sterilization is to excite and separate the e^-/h^+ pairs via illumination; the photoinduced electrons and/or holes then inactivate the bacteria by directly or indirectly inflicting oxidative damage on their organs (through the formation of $•O_2^-$, •OH, etc.). Hence, the disinfection efficiency of materials closely depends on the properties that influence the generation and separation of e^-/h^+ pairs, e.g., the surface area, the band gap and the surface morphology, as reported for other photocatalytic processes.

In the case of g-C_3N_4, Huang et al. [33] found that mesoporous g-C_3N_4 synthesized using the hard template method can inactivate most of the bacteria (e.g., *E. coli* K-12) within 4 h, owing to its large surface area, which allows more active sites exposed on the surface to produce h^+ for bacterial disinfection. To support that the inactivation of bacteria is caused by photocatalysis, Xu et al. [34] conducted a dark contrasting experiment using a porous g-C_3N_4 nanosheet (PCNS) as the photocatalyst and *E. coli* as the model bacteria; they found that the adsorption of *E. coli* on PCNS reaches equilibrium within 1 h and about 85.5% of *E. coli* survive after 4 h, while nearly 100% of *E. coli* are killed by PCNS within 4 h under visible-light irradiation. This demonstrates that the PCNS has little toxic effect on *E. coli* and the disinfection is mainly caused by the electrons or holes induced from PCNS under light irradiation.

In addition to bacterial infection, viral outbreaks, including SARS, bird flu, Ebola and the recent COVID-19, are also important events related to human health, and they are generally more resistant than bacteria to conventional disinfection due to their small size. Thus, the inactivation of viruses normally requires strong oxidative agents. g-C_3N_4-based materials have good photocatalytic reactivity to produce strong oxidative agents, e.g., $•O_2^-$ and •OH; hence, they are potential photocatalysts for virus inactivation. It has been reported that phage MS_2 can be completely inactivated by g-C_3N_4 under visible-light irradiation within 360 min [35], and the main active species for the reaction are $•O_2^-$ and •OH. The loss of

protein triggers the leakage and rapid destruction of internal components, and ultimately leads to the death of the virus without regrowth.

References

1. Xu, Q.; Zhang, L.; Cheng, B.; Fan, J.; Yu, J. S-Scheme Heterojunction Photocatalyst. Chem 2020, 6, 1543–1559.
2. Low, J.; Yu, J.; Jaroniec, M.; Wageh, S.; Al-Ghamdi, A.A. Heterojunction Photocatalysts. Adv. Mater. 2017, 29, 1601694.
3. Shi, J.; Zheng, B.; Mao, L.; Cheng, C.; Hu, Y.; Wang, H.; Li, G.; Jing, D.; Liang, X. MoO3/g-C3N4 Z-scheme (S-scheme) system derived from MoS2/melamine dual precursors for enhanced photocatalytic H2 evolution driven by visible light. Int. J. Hydrogen Energy 2021, 46, 2927–2935.
4. Li, W.; Da, P.; Zhang, Y.; Wang, Y.; Zheng, G. WO nanoflakes for enhanced photoelectrochemical conversion. ACS Nano 2014, 8, 11770–11777.
5. Bai, Y.; Ye, L.; Wang, L.; Shi, X.; Wang, P.; Bai, W. A dual-cocatalyst-loaded Au/BiOI/MnOx system for enhanced photocatalytic greenhouse gas conversion into solar fuels. Environ. Sci. Nano. 2016, 3, 902–909.
6. Chen, X.; Zhu, K.; Wang, P.; Sun, G.; Yao, Y.; Luo, W.; Zou, Z. Reversible Charge Transfer and Adjustable Potential Window in Semiconductor/Faradaic Layer/Liquid Junctions. iScience 2020, 23, 100949.
7. Jahurul Islam, M.; Amaranatha Reddy, D.; Han, N.S.; Choi, J.; Song, J.K.; Kim, T.K. An oxygen-vacancy rich 3D novel hierarchical MoS2/BiOI/AgI ternary nanocomposite: Enhanced photocatalytic activity through photogenerated electron shuttling in a Z-scheme manner. Phys. Chem. Chem. Phys. 2016, 18, 24984–24993.
8. Wang, N.; Wu, L.; Li, J.; Mo, J.; Peng, Q.; Li, X. Construction of hierarchical Fe2O3@MnO2 core/shell nanocube supported C3N4 for dual Z-scheme photocatalytic water splitting. Sol. Energy Mater. Sol. Cells 2020, 215, 110624.
9. Chang, X.; Wang, T.; Gong, J. CO2 photo-reduction: Insights into CO2 activation and reaction on surfaces of photocatalysts. Energy Environ. Sci. 2016, 9, 2177–2196.
10. He, Y.; Wang, Y.; Zhang, L.; Teng, B.; Fan, M. High-efficiency conversion of CO2 to fuel over ZnO/g-C3N4 photocatalyst. Appl. Catal. B Environ. 2015, 168–169, 1–8.
11. Nie, N.; Zhang, L.; Fu, J.; Cheng, B.; Yu, J. Self-assembled hierarchical direct Z-scheme g-C3N4/ZnO microspheres with enhanced photocatalytic CO2 reduction performance. Appl. Surf. Sci. 2018, 441, 12–22.
12. Bhosale, R.; Jain, S.; Vinod, C.P.; Kumar, S.; Ogale, S. Direct Z-Scheme g-C3N4/FeWO4 Nanocomposite for Enhanced and Selective Photocatalytic CO2 Reduction under Visible Light. ACS Appl. Mater. Interfaces 2019, 11, 6174–6183.
13. Ge, L.; Peng, Z.; Wang, W.; Tan, F.; Wang, X.; Su, B.; Qiao, X.; Wong, P.K. g-C3N4/MgO nanosheets: Light-independent, metal-poisoning-free catalysts for the activation of hydrogen peroxide to degrade organics. J. Mater. Chem. A 2018, 6, 16421–16429.
14. Fan, J.; Qin, H.; Jiang, S. Mn-doped g-C3N4 composite to activate peroxymonosulfate for acetaminophen degradation: The role of superoxide anion and singlet oxygen. Chem. Eng. J. 2019, 359, 723–732.
15. Ding, X.; Xiao, D.; Ji, L.; Jin, D.; Dai, K.; Yang, Z.; Wang, S.; Chen, H. Simple fabrication of Fe3O4/C/g-C3N4 two-dimensional composite by hydrothermal carbonization approach with enhanced photocatalytic performance under visible light. Catal. Sci. Technol. 2018, 8, 3484–3492.
16. Zou, X.; Dong, Y.; Li, S.; Ke, J.; Cui, Y.; Ou, X. Fabrication of V2O5/g-C3N4 heterojunction composites and its enhanced visible light photocatalytic performance for degradation of gaseous ortho-dichlorobenzene. J. Taiwan Inst. Chem. E. 2018, 93, 158–165.
17. Katsumata, K.-i.; Motoyoshi, R.; Matsushita, N.; Okada, K. Preparation of graphitic carbon nitride (g-C3N4)/WO3 composites and enhanced visible-light-driven photodegradation of acetaldehyde gas. J. Hazard. Mater. 2013, 260, 475–482.
18. Wang, S.; Ding, X.; Zhang, X.; Pang, H.; Hai, X.; Zhan, G.; Zhou, W.; Song, H.; Zhang, L.; Chen, H.; et al. In Situ Carbon Homogeneous Doping on Ultrathin Bismuth Molybdate: A Dual-Purpose Strategy for Efficient Molecular Oxygen Activation. Adv. Funct. Mater. 2017, 27, 1703923.
19. Xu, X.; Geng, A.; Yang, C.; Carabineiro, S.A.C.; Lv, K.; Zhu, J.; Zhao, Z. One-pot synthesis of La–Fe– composites as photo-Fenton catalysts for highly efficient removal of organic dyes in wastewater. Ceram. Int. 2020, 46, 10740–10747.

20. Xu, Q.; Zhao, P.; Shi, Y.-K.; Li, J.-S.; You, W.-S.; Zhang, L.-C.; Sang, X.-J. Preparation of a g-C3N4/Co3O4/Ag2O ternary heterojunction nanocomposite and its photocatalytic activity and mechanism. New J. Chem. 2020, 44, 6261–6268.
21. She, X.; Xu, H.; Wang, H.; Xia, J.; Song, Y.; Yan, J.; Xu, Y.; Zhang, Q.; Du, D.; Li, H. Controllable synthesis of CeO2/g-C3N4 composites and their applications in the environment. Dalton T. 2015, 44, 7021–7031.
22. Chen, H.Y.; Qiu, L.G.; Xiao, J.D.; Ye, S.; Jiang, X.; Yuan, Y.P. Inorganic–organic hybrid NiO–g-C3N4 photocatalyst for efficient methylene blue degradation using visible light. RSC Adv. 2014, 4, 22491.
23. Jiang, Z.; Jiang, D.; Yan, Z.; Liu, D.; Qian, K.; Xie, J. A new visible light active multifunctional ternary composite based on TiO2–In2O3 nanocrystals heterojunction decorated porous graphitic carbon nitride for photocatalytic treatment of hazardous pollutant and H2 evolution. Appl. Catal. B Environ. 2015, 170–171, 195–205.
24. Zhang, Y.; Xu, M.; Li, H.; Ge, H.; Bian, Z. The enhanced photoreduction of Cr(VI) to Cr(III) using carbon dots coupled TiO2 mesocrystals. Appl. Catal. B Environ. 2017, 226, 213–219.
25. Song, X.-Y.; Chen, Q.-L. Facile preparation of g-C3N4/Bi2WO6 hybrid photocatalyst with enhanced visible light photoreduction of Cr(VI). J. Nanopart. Res. 2019, 21, 183.
26. Ali, T.; Muhammad, N.; Qian, Y.; Liu, S.; Wang, S.; Wang, M.; Qian, T.; Yan, C. Recent advances in material design and reactor engineering for electrocatalytic ambient nitrogen fixation. Mater. Chem. Front. 2022, 6, 843–879.
27. Zhu, J.; Wei, Y.; Chen, W.; Zhao, Z.; Thomas, A. Graphitic carbon nitride as a metal-free catalyst for NO decomposition. Chem. Commun. 2010, 46, 6965–6967.
28. Sano, T.; Tsutsui, S.; Koike, K.; Hirakawa, T.; Teramoto, Y.; Negishi, N.; Takeuchi, K. Activation of graphitic carbon nitride (g-C3N4) by alkaline hydrothermal treatment for photocatalytic NO oxidation in gas phase. J. Mater. Chem. A 2013, 1, 6489–6496.
29. Wang, Z.; Guan, W.; Sun, Y.; Dong, F.; Zhou, Y.; Ho, W.-K. Water-assisted production of honeycomb-like g-C3N4 with ultralong carrier lifetime and outstanding photocatalytic activity. Nanoscale 2015, 7, 2471–2479.
30. Shi, L.; Liang, L.; Wang, F.; Ma, J.; Sun, J. Polycondensation of guanidine hydrochloride into a graphitic carbon nitride semiconductor with a large surface area as a visible light photocatalyst. Catal. Sci. Technol. 2014, 4, 3235–3243.
31. Wang, W.; Huang, G.; Yu, J.C.; Wong, P.K. Advances in photocatalytic disinfection of bacteria: Development of photocatalysts and mechanisms. J. Environ. Sci. 2015, 34, 232–247.
32. Tadashi, M.; Ryozo, T.; Toshiaki, N.; Hitoshi, W. Photoelectrochemical sterilization of microbial cells by semiconductor powders. FEMS Microbiol. Lett. 1985, 29, 211–214.
33. Huang, J.; Ho, W.; Wang, X. Metal-free disinfection effects induced by graphitic carbon nitride polymers under visible light illumination. Chem. Commun. 2014, 50, 4338–4340.
34. Xu, J.; Wang, Z.; Zhu, Y. Enhanced Visible-Light-Driven Photocatalytic Disinfection Performance and Organic Pollutant Degradation Activity of Porous g-C3N4 Nanosheets. ACS Appl. Mater. Interfaces 2017, 9, 27727–27735.
35. Li, Y.; Zhang, C.; Shuai, D.; Naraginti, S.; Wang, D.; Zhang, W. Visible-light-driven photocatalytic inactivation of MS2 by metal-free g-C3N4: Virucidal performance and mechanism. Water Res. 2016, 106, 249–258.